Crossover from 2D to 3D in a weakly interacting Fermi gas

P. Dyke,[1] E. D. Kuhnle,[1] S. Whitlock,[1,2] H. Hu,[1] M. Mark,[1] S. Hoinka,[1] M. Lingham,[1] P. Hannaford,[1] and C. J. Vale[1]

[1]*ARC Centre of Excellence for Quantum-Atom Optics,*
Centre for Atom Optics and Ultrafast Spectroscopy,
Swinburne University of Technology, Melbourne 3122, Australia
[2]*Physikalisches Institut, Universität Heidelberg, Philosophenweg 12, 69120 Heidelberg, Germany*
(Dated: November 8, 2010)

We have studied the transition from two to three dimensions in a low temperature weakly interacting ^{6}Li Fermi gas. Below a critical atom number, N_{2D}, only the lowest transverse vibrational state of a highly anisotropic oblate trapping potential is occupied and the gas is two-dimensional. Above N_{2D} the Fermi gas enters the quasi-2D regime where shell structure associated with the filling of individual transverse oscillator states is apparent. This dimensional crossover is demonstrated through measurements of the cloud size and aspect ratio versus atom number.

Two-dimensional (2D) ensembles of strongly correlated fermions occur in a number of important settings including high temperature superconductors [1] and ^{3}He films [2]. Ultracold neutral atoms provide new opportunities to explore such systems where the dimensionality and interactions can be precisely controlled [3]. To date great progress has been made through investigations of the Bose-Einstein condensate (BEC) to Bardeen-Cooper-Schrieffer (BCS) superfluid crossover [4–10] in gases free to move in three spatial dimensions. Freezing the motion in one or more dimensions through tight confinement can have dramatic consequences. For instance in a homogeneous 2D Bose gas there is no Bose-Einstein condensation at finite temperature as phase fluctuations destroy long range order [11, 12]. However, as shown by Berezinskii [13] and Kosterlitz and Thouless [14], a system of interacting particles can form a (BKT) superfluid. Two-dimensional gases of fermionic atoms are poised to provide new insights into 2D superfluidity and can also display mesoscopic phenomena such as shell structure [15–17] which arises due to Pauli exclusion.

In this letter we study the crossover from 2D to 3D in an optically trapped ^{6}Li degenerate Fermi gas. The scaling of the cloud width with atom number in both the tight and weakly confined directions changes dramatically through the crossover. We also see clear indications of the characteristic shell-structure associated with the filling of discrete energy levels; a feature which is most pronounced when looking at the aspect ratio of the cloud. The experimentally observed structure agrees well with theoretical predictions for an ideal Fermi gas.

Achieving the 2D regime in a Fermi gas requires that the Fermi energy, E_F, and temperature, T, are sufficiently low that excitations in the restricted dimension are forbidden. Theoretical studies have shown that quasi-2D systems are a promising route towards fermionic superfluidity [18]. The possibility of observing a 2D BKT superfluid with fermions [19, 20] has recently emerged. The BEC-BCS crossover displays a different character in

balanced [21] and in imbalanced [22] 2D systems. This is manifest through the existence of a two-body bound state for arbitrarily weak attractive interactions in 2D [23–25], making 2D Fermi gases a rich field for study.

The first demonstration of an ultracold 2D Fermi gas was achieved using ^{40}K atoms confined in a 1D optical lattice [26]. Restricting dimensions with an optical lattice was shown to shift the position of a p-wave Feshbach resonance in ^{40}K [27]. In 2009 Du *et al.* [28] studied inelastic collisions in a quasi-2D Fermi gas and more recently Martiyanov *et al.* produced an array of 2D gases using ^{6}Li atoms in an optical lattice [29]. Experiments in lattices produce multiple 2D clouds that can be imaged simultaneously giving better signal to noise for bulk measurements. However, the properties of individual clouds in lattices cannot be easily measured. In the tightly confined direction the cloud size is typically sub-micron and hence well below the resolution limit of nearly all imaging systems. We overcome this limitation by using a single 2D cloud.

The transition from 2D to 3D is readily understood by considering an ideal Fermi gas confined in an harmonic trapping potential

$$V(x,y,z) = \frac{1}{2}m(\omega_x x^2 + \omega_y y^2 + \omega_z z^2), \qquad (1)$$

where m is the mass of the atoms and $\omega_{x,y,z}$ are the trapping frequencies in the x, y and z directions, respectively. For simplicity, we consider the radially symmetric case $\omega_x = \omega_y = \omega_r$ and an oblate geometry where $\omega_z \gg \omega_r$. In 2D the Fermi energy is given by $E_{F,2D} = \sqrt{2N}\hbar\omega_r$ where N is the atom number. In 3D the Fermi energy is $E_{F,3D} = (6N)^{1/3}\hbar\bar{\omega}$ where $\bar{\omega} = (\omega_x\omega_y\omega_z)^{1/3}$ is the geometric mean trapping frequency.

At zero temperature, the Fermi radii in both 2D and 3D are found simply from the Fermi energy. In 3D this gives the well known result $R_{F,r_i} = (48N)^{1/6}\sqrt{\hbar\bar{\omega}/(m\omega_{r_i}^2)}$, where $r_i = x, y, z$. In contrast when the gas is confined to two dimensions (when $E_F \ll \hbar\omega_z$) the width in the tightly confined direction is

fixed by the size of the harmonic oscillator ground state $a_z = \sqrt{\hbar/(m\omega_z)}$. In the radial directions, however, the Fermi radius is

$$R_{F,r} = (8N)^{1/4}\sqrt{\frac{\hbar}{m\omega_r}}. \quad (2)$$

This $N^{1/4}$ growth is more rapid than in 3D as two phase space degrees of freedom (z, p_z) are no longer accessible. As the Fermi energy depends on the atom number we define a critical number N_{2D} below which atoms populate only the lowest transverse vibrational state at $T = 0$. This is found by counting the number of single particle states with energy less than the lowest energy state with one transverse excitation. Labelling harmonic oscillator states by the vibrational quantum numbers n_x, n_y and n_z and defining the trap aspect ratio as $\lambda = \omega_z/\omega_r$ the energy of an arbitrary state is given by

$$E(n_x, n_y, n_z) = \hbar\omega_r \left[n_x + n_y + 1 + \lambda(n_z + 1/2)\right]. \quad (3)$$

The number of $(n_z = 0)$ states with energy less than the $(n_x = n_y = 0, n_z = 1)$ state is the maximum number of particles that can be accommodated while remaining in the true 2D regime. These states satisfy $n_x + n_y < \lambda$, so N_{2D} is given by

$$N_{2D} = \sum_{n_x=0}^{\lambda-1}\sum_{n_y=0}^{(\lambda-n_x-1)} 1 = \frac{\lambda}{2}(\lambda+1). \quad (4)$$

This critical number increases with the square of the trap aspect ratio. In the experiments that follow, we work in a trap with $\lambda \approx 60$ corresponding to $N_{2D} \approx 1800$.

As well as the critical atom number it is also possible to calculate the root mean square (rms) cloud width $\sigma_{r_i} = \sqrt{\langle r_i^2 \rangle}$. This provides a model independent measure of the cloud size applicable at both zero and finite temperatures. In the case of an ideal Fermi gas, σ_{r_i} can be found by summing the squared wavefunctions of the individual oscillator states to obtain a full density profile $n(x, y, z)$. These profiles can then be integrated over two spatial dimensions to produce a line profile $n(r_i)$ from which the second moment can be evaluated $\langle r_i^2 \rangle = \int n(r_i)r_i^2 dr_i / \int n(r_i)dr_i = \sigma_{r_i}^2$.

To create a 2D Fermi gas, we begin with an evaporatively cooled cloud of approximately $N = 10^5$ ^{6}Li atoms in each of the lowest two spin states $|F = 1/2, m_F = \pm1/2\rangle$ in a single beam optical dipole trap at a temperature of $T \approx 0.1\,T_F$ [30, 31]. To vary the final atom number we continue the evaporation by further lowering the dipole trap power so that atoms are spilled while maintaining the cloud at the lowest possible temperature. The final stage of the evaporation takes place at 834 G where two-body scattering is unitarity-limited [32].

Next we adiabatically ramp on the 2D optical trap, which is formed by a cylindrically focussed Gaussian beam ($\lambda = 1075$ nm) propagating along the y-direction
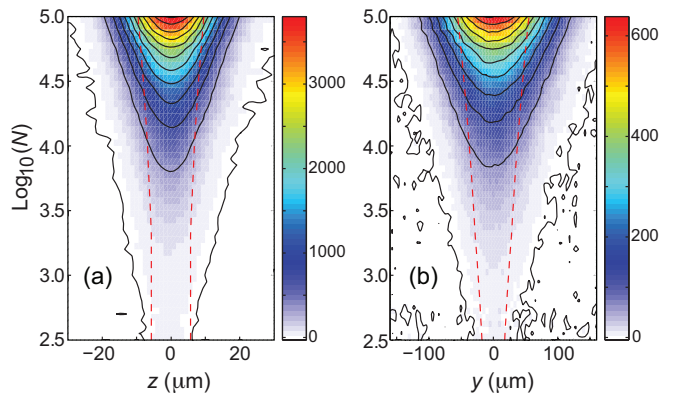

Figure 1. Contour plots of the measured 1D density profiles as a function of atom number in both the tight (a) and weakly confined (b) directions after 500 μs expansion. Solid black lines are contours of equal density and the dashed red lines show the zero temperature rms cloud width. The color bar indicates line density in units of atoms/μm.

with $1/e^2$ waists of $w_z = 8\,\mu$m and $w_x = 400\,\mu$m in 200 ms. Similar trapping configurations have been used to study 2D Bose gases [33, 34]. Once the trap is fully on, the first beam used for evaporation is adiabatically ramped down in 200 ms leaving the atoms in the 2D trap. Confinement in the y-direction of the 2D trap is achieved by the short Rayleigh length associated with the 8 μm waist. Additional harmonic confinement in the x and y-directions is provided by residual curvature of the Feshbach magnetic field. The 2D trapping frequencies were measured to be $\omega_z/2\pi = 2800$ Hz and $\omega_r/2\pi = 47$ Hz ($\omega_x \sim \omega_y \equiv \omega_r$) giving an aspect ratio of approximately 60. The final stage of the preparation involves adiabatically ramping the magnetic field to 992 G where the s-wave scattering length is $a_s = -4300a_0$ (a_0 is the Bohr radius) and the cloud is imaged after 500 μs time of flight. Cloud temperatures in the 2D trap are difficult to ascertain due to the lack of an analytic model in the interacting quasi-2D regime. However, in the 2D trap we expect $T < 0.1\,T_F$ due to the adiabatic sweep of the magnetic field and the deep evaporation used to prepare the low atom number clouds.

To demonstrate the crossover from 2D to 3D we measure the rms cloud radii in the tight and weakly confined directions as a function of the atom number. In the tightly confined z-direction the cloud width in trap ($a_z \sim \sqrt{\hbar/(m\omega_z)} \approx 770$ nm) is much smaller than the resolution of our imaging system, so a short time of flight (500 μs) is allowed before imaging. This time was chosen to be long compared to the inverse trapping frequency in the z-direction ($1/\omega_z = 57\,\mu$s) and short compared to the inverse trapping frequencies in the radial directions ($1/\omega_y = 3.4$ ms). The measured spatial distribution in the radial dimension will thus be very close to the in-trap distribution.

The imaging beam propagates roughly along the (radial) x-direction, so we obtain two-dimensional density profiles $n(z, y)$. From these we generate line profiles $n(z)$, $n(y)$ by integrating over the other dimension. Absorption images are processed using a fringe removal algorithm [35] to optimise the image quality. Figure 1(a) and (b) show the measured line-densities as a function of atom number for gases at 992 G ($a_s = -4300a_0$) in both the tight and weakly confined directions, respectively. The plots consist of approximately 50 profiles; each profile is the average of several images binned according to N. The dashed red lines show the scaled predictions for the zero temperature rms radius for an ideal Fermi gas and the solid lines are contours of equal density.

In order to compare these data with theory, we evaluate the rms cloud widths from the profiles in Fig. 1. Figure 2 (main panel) shows the rms width in the y-direction (σ_y) versus atom number. Data points are the experimentally measured widths and the solid line is the calculated width for an ideal $T = 0$ Fermi gas. The theoretical curve has been scaled by a factor of 1.1 to provide the best agreement with the experimental data for low atom numbers ($N < 5000$) where interactions play a minor role. We attribute this scaling to a combination of finite imaging resolution and nonzero cloud temperature. The data points follow the predicted growth rate at low atom numbers, but drop below the theory at high numbers (densities), where the attractive interactions become more significant. Below $N_{2D} = 1800$, a least squares fit to the experimental data shows that the width grows as $N^{0.28\pm0.05}$, in agreement with the predicted $N^{0.25}$ scaling for an ideal gas. Above $N = 5000$, a fit to the data yields a power law dependence of $N^{0.148\pm0.004}$, below the ideal gas prediction of $N^{0.174}$, due to interactions. For the lowest atom numbers shown in this plot ($N \approx 800$) the interaction parameter $1/(k_F a_s) = -2.3$, where k_F is the Fermi wave-vector. For the highest numbers ($N \approx 10^5$) the gas is approaching the strongly interacting regime, $1/(k_F a_s) = -1.0$, and the ideal gas picture will fail.

The inset of Fig. 2 shows the measured widths in the tightly confined z-direction. The theoretical width has been scaled by $b\sqrt{1 + \omega_z^2 t^2} \cong b\omega_z t$ to account for the 500 μs expansion time ($\omega_z^2 t^2 \approx 80 \gg 1$). The value of b which provides the best agreement with the data is 1.17. This differs from the 1.1 scaling found for the radial direction suggesting that the expansion may not be simply ballistic. Below N_{2D} the width scales with $N^{0.07\pm0.04}$ in reasonable agreement with the N^0 prediction for the ideal gas. Finite temperature may lead to some population of the ($n_z = 1$) state for atom numbers below N_{2D}. For $N > 5000$ the measured width scales as $N^{0.132\pm0.005}$, in excellent agreement with the ideal gas result of $N^{0.135}$. We note that the measured exponents may be influenced by interaction dependent expansion dynamics in the z-direction [36]. The calculated exponent for the non-interacting gas is below the
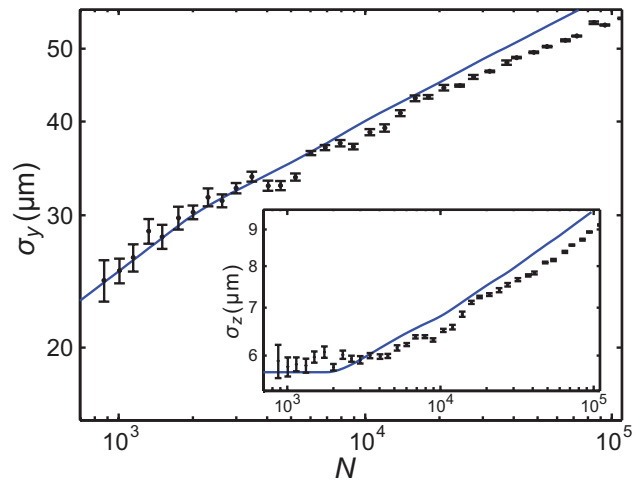

Figure 2. Measured rms cloud widths (data points) and the theoretical predictions for an ideal $T = 0$ Fermi gas (solid lines). Radial cloud width is plotted in the main panel and the inset shows the transverse cloud width after 500 μs expansion. Theoretical curves have been scaled as described in the text.

true 3D value of $1/6$ as the data in the range considered here lies in the quasi-2D regime where shell structure influences the widths. The theoretical curves in Fig. 2 display the characteristic steps in gradient due to shell structure although it is difficult to identify these steps in the experimental data here.

To further investigate the emergence of shell structure we examine the cloud aspect ratio, $\kappa = \sigma_z/\sigma_y$. Shell structure will be more prominent in measurements of κ as the filling of a new transverse state begins in states with the lowest radial quantum numbers. Hence an increase in the transverse cloud size will correlate with a decrease in the growth rate of the radial size. In the 3D limit, the cloud aspect ratio will be constant but in 2D and quasi-2D κ will show a strong dependence on the atom number. Additionally, as κ is given by the ratio of two measured quantities, the influence of certain experimental systematics (for example finite imaging resolution and shot to shot temperature variations) can be reduced.

In Fig. 3 (main panel) we plot the aspect ratio of the cloud along with the theoretical predictions for a zero temperature ideal Fermi gas. The agreement between theory and experiment is very good and the large change in aspect ratio with N clearly demonstrates departure from 3D behavior. Only at the highest atom numbers does the aspect ratio begin to level off indicating broad coverage of the 2D and quasi-2D regimes. The dashed vertical lines indicate the calculated atom numbers at which new transverse states become accessible for a zero temperature ideal gas. At low N, the aspect ratio decays steadily with increasing atom number, before a step occurs at N_{2D} corresponding to occupation of the first transverse excited state. The inset of Fig. 3 shows the gradient $d\kappa/dN$ of the theoretical and experimental as-
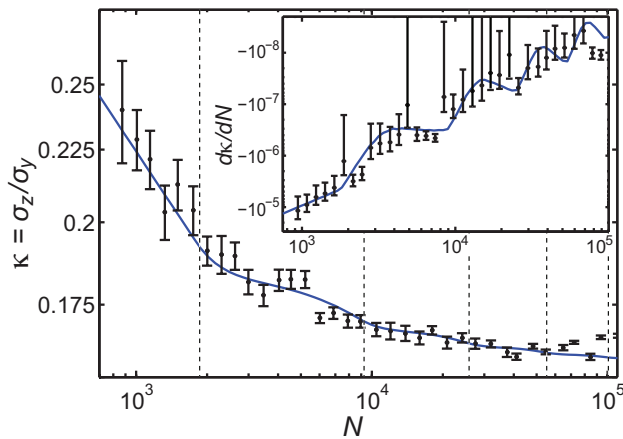
Figure 3. Aspect ratio of the cloud through the 2D to 3D crossover (data points) and theoretical predictions for an ideal Fermi gas (solid line). Dashed lines indicate the predicted location of the steps associated with the occupation of the successive transverse oscillator states. Inset: Gradient of the experimental and theoretical aspect ratios showing the signature of shell filling.

pect ratios which show the signatures of shell structure more clearly. The steps in the theoretical curve in the inset plot correspond to the dashed lines in the main panel. The experimental gradients were evaluated numerically and smoothed with a five-point moving average. Both the measured aspect ratio and gradient follow the theoretical predictions, with indications of shell structure present in the experimental data for $N \lesssim 10,000$ corresponding to occupation of the ground and first transverse excited states. For larger N the data lie close to the theoretical line but the shell structure is unresolved. For atom numbers less than 10,000 the interaction parameter $1/(k_F a_s)$ remains below -1.5, so the ideal gas theory provides a reasonable description of this situation.

This work provides the first quantitative study of the transition from 2D to quasi-2D and 3D in a Fermi gas. The weakly interacting Fermi gas used for these studies behaves similarly to a non-interacting gas, particularly at low atom numbers where shell structure associated with the filling of individual transverse oscillator states becomes apparent. These data were obtained in the regime where confinement induced scattering resonances should not affect the measurements ($a_s < a_z$) but these phenomena can readily be accessed at larger scattering lengths closer to the Feshbach resonance [24, 37, 38]. This work opens the way to further investigations of the phase diagram of 2D and quasi-2D Fermi gases as a function of the 3D scattering length and temperature.

[1] A. J. Leggett, Nature Phys. **2**, 134 (2006).
[2] M. Neumann, J. Nyeki, B. Cowan, and J. Saunders, Science **317**, 1356 (2007).
[3] I. Bloch, J. Dalibard, and W. Zwerger, Rev. Mod. Phys. **80**, 885 (2008).
[4] S. Jochim *et al.* Science **302**, 2101 (2003).
[5] M. Greiner, C. A. Regal, and D. S. Jin, Nature **426**, 537 (2003).
[6] T. Bourdel *et al.*, Phys. Rev. Lett. **93**, 050401 (2004).
[7] M. W. Zwierlein *et al.*, Nature **435**, 1047 (2005).
[8] J. Kinast *et al.*, Science **307**, 1296 (2005).
[9] G. B. Partridge *et al.*, Phys. Rev. Lett. **95**, 020404 (2005).
[10] S. Giorgini, L. P. Pitaevskii, and S. Stringari, Rev. Mod. Phys. **80**, 1215 (2008).
[11] N. D. Mermin, and H. Wagner, Phys. Rev. Lett. **17**, 1133 (1966).
[12] P. C. Hohenberg, Phys. Rev. **158**, 383 (1967).
[13] V. L. Berezinskii, Sov. Phys. JETP **32**, 493 (1971).
[14] J. Kosterlitz, and D. Thouless, J. Phys. C **6**, 1181 (1973).
[15] J. Schneider, and H. Wallis, Phys. Rev. A **57**, 1253 (1998).
[16] P. Vignolo, and A. Minguzzi, Phys. Rev. A **67**, 053601 (2003).
[17] E. J. Mueller, Phys. Rev. Lett. **93**, 190404 (2004).
[18] D. S. Petrov, M. A. Baranov, and G. V. Shlyapnikov, Phys. Rev. A **67**, 031601(R) (2003).
[19] W. Zhang, G. D. Lin, and L.-M. Duan, Phys. Rev. A **78**, 043617 (2008).
[20] M. Iskin, and C. A. R. Sá de Melo, Phys. Rev. Lett. **103**, 165301 (2009).
[21] W. Zhang, G. D. Lin, and L.-M. Duan, Phys. Rev. A **77**, 063613 (2008).
[22] J. Tempere, S. N. Klimin, and J. T. Devreese, Phys. Rev. A **79**, 053637 (2009).
[23] M. Randeria, J.-M. Duan, and L.-Y. Shieh Phys. Rev. B **41**, 327 (1990)
[24] D. S. Petrov, and G. V. Shlyapnikov, Phys. Rev. A **64**, 012706 (2001).
[25] L. Salasnich, Phys. Rev. A **76**, 015601 (2007).
[26] G. Modugno *et al.*, Phys. Rev. A **68**, 011601 (2003).
[27] K. Günter, *et al.*, Phys. Rev. Lett. **95**, 230401, (2005).
[28] X. Du, Y. Zhang, and J. E. Thomas, Phys. Rev. Lett **102**, 250402 (2009).
[29] K. Martiyanov, V. Makhalov, and A. Turlapov, Phys. Rev. Lett. **105**, 030404 (2010).
[30] J. Fuchs *et al.*, J. Phys. B: At. Mol. Opt. Phys. **40**, 4109 (2007).
[31] G. Veeravalli, E. Kuhnle, P. Dyke, and C. J. Vale, Phys. Rev. Lett. **101**, 250403 (2008).
[32] W. Ketterle, and M. W. Zwierlein, Ultracold Fermi Gases, Proceedings of the International School of Physics "Enrico Fermi", Course CLXIV, Varenna, 2006, edited by M. Inguscio, W. Ketterle, and C. Salomon (IOS Press, Amsterdam, 2008).
[33] A. Görlitz *et al.*, Phys. Rev. Lett. **87**, 130402 (2001).
[34] P. Cladé *et al.*, Phys. Rev. Lett. **102**, 170401(2009).
[35] C. F. Ockeloen, A. F. Tauschinsky, R. J. C. Spreeuw, S. Whitlock, arXiv:1007.2136v1[physics.atom-ph] (2010).
[36] C. Menotti, P. Pedri, and S. Stringari, Phys. Rev. Lett. **89**, 250402 (2002).
[37] T. Bergeman, M. G. Moore, and M. Olshanii, Phys. Rev.

Lett. **91**, 163201 (2003).

[38] E. Haller *et al.*, Phys. Rev. Lett. **104**, 153203 (2010).